



Joining Dissimilar Material Pairs by Mechanical Locking Method (MLM)

Serdar Mercan¹

Received: 25 April 2021 / Revised: 24 August 2021 / Accepted: 1 October 2021 / Published online: 22 October 2021
© Korean Society for Precision Engineering 2021

Abstract

Several methods that have been used in joining material pairs with different properties share many disadvantages. To overcome these disadvantages, the current study introduces mechanical locking method (MLM), which is a new and environmentally friendly method. This method can prevent many problems, especially those related to chemical incompatibility in practical applications. The method helps materials with physical and chemical incompatibilities join successfully. The only limitation in the joining process is that one of the materials must melt. When this criterion is met, ceramics can be joint with metals, ferrous-based materials can be joint with non-ferrous metals and other types of materials. This study used two different metal alloys, namely plain carbon steel and brass (CuZn30) for MLM as mold metal and reshaping metal, respectively. MLM process resulted in a successful joining for steel-brass alloys. Joint material pairs were examined using microstructural methods and mechanical properties. The study used the tensile test to evaluate the mechanical properties of joint metals, and used Vickers indentation for hardness measurement. The researcher conducted Scanning Electron Microscope (SEM) investigations for possible interface reactions and re-formed grain structures for both alloys.

Keywords Mechanical locking method · AISI1040/CuZn30 · Joining · Mechanical · Metallurgical

1 Introduction

Brass is an alloy of Cu and Zn. The proportion of Zn in the alloy can vary along a wide range from 5 to 45wt%. Its machinability, good corrosion resistance, long-lasting fatigue resistance combined with high electrical and thermal conductivity make brass an important engineering material for structural and industrial engineering applications. However, relatively low hardness of brass limits its application in a wide range in the industry [1]. Therefore, joining it with a material with high hardness can increase application areas of brass.

Joining the material pairs with different physical and chemical properties such as steel and brass, which are examined in this research, using welding methods is almost impossible [2]. This is mainly attributed to the large differences in thermophysical properties between copper and steel, such as melting point, thermal conductivity,

expansion coefficient and shrinkage rate [3]. Joining dissimilar metals may lead to welding defects such as inclusions, cracking, hot tear, porosity and coarse grains in HAZ which produces poor mechanical properties of the joints [4]. Material pairs that contain chemical and thermophysical incompatibilities and cannot be joined using traditional welding methods are joined using a new joining method, MLM. Thus, bimetallic applications and different material pairs can be used together. Many material types such as ferrous materials, non-ferrous metals, composite materials and ceramic materials can be joined with each other using MLM. In MLM, the joining process involves two metals, and one of them is referred to as mold metal, and the other one is referred to as deforming or reshaped metal or alloy. The part with high melting temperature and mechanical properties is selected as a mold part, and a conical channel or T channel is opened on it. Reshaped material should have a plastic deformation property [5]. After these preliminary preparations, a system is designed to ensure the friction of the part to be reshaped by rotating in the channel opened in the mold part and to create axial pressure between them. This system is designed to use the heat generated by converting mechanical energy into thermal energy and to produce plastic deformation. The

✉ Serdar Mercan
smsmercan@gmail.com

¹ Department of Mechatronics Engineering, Faculty of Technology, Sivas Cumhuriyet University, 58140 Sivas, Turkey

first friction movement continues until it reaches plastic deformation temperature. Heat is released on the friction surfaces and the reshaped part starts to pile up with the effect of axial pressure. When the piled material takes the form of a mold, the friction movement suddenly stops and a mechanical joint that cannot be removed is achieved [5, 6]. Flanges, which are formed as a result of the friction, are used to provide the connection. The joint is not produced using a welded bonding but produced using a negative channel opened on the mold part. While producing the joint, the sudden stopping of the friction movement prevents the possible regional connections that may occur at the interface. An atomic bonding is not expected at the interface, but a drop and/or regional joints that may occur affect the mechanical properties of the joint positively.

MLM can be easily implemented using suitable tools such as lathe devices, classical friction welding machines and milling machines. The parameters used in the MLM method are rotational speed and axially applied friction pressure. Depending on the choice of the machine used in the application of the method, a pressure-generating feed can be used instead of friction pressure. On the other hand, mold channel depth, joint angle and channel corner radius, which have significant effects on the joint quality, should be determined in accordance with the material properties [5, 6]. In the process, there is no need for upset pressure because the stepped surfaces of the parts continue until they touch each other. The length of the process is determined naturally depending on the feed rate or applied axial pressure [6].

The most important limitation of the MLM method is that the mechanical properties of the plastic deformation material are adversely affected due to the intense deformation. Therefore, in MLM, which is a new method, all parameters of the method should be examined in detail and harmonized with each other. Similarly, determining the parameters in different material groups and investigating the application areas will enable the method to be used in industrial applications in the near future.

The method is similar to plastic forming, friction welding (FW) and friction stir welding (FSW) in terms of process steps. However, flange occurs after the process is over in FW and FSW methods. While these flanges are cleaned and disposed of after joining in FW and FSW methods, no waste material occurs in MLM. With MLM, the initial section of the object is transformed into another section, and mass loss and composition change do not occur in the material during this process. Especially if the mold part is shaped by the casting method, joining is completed in an environmentally friendly manner without creating waste, and no additional process is needed.

Literature review was completed by considering FW, FSW and plastic shaping methods, which are similar to MLM method.

Kumar et al. [7] used the FW method while joining steel materials and reported that three different structures were formed in the microstructure and grain refinement occurred. They reported that the three different regions were formed in the microstructure; namely the junction interface, radial plastic flow (RPF), axial plastic flow (APF), and thermomechanically affected zone (TMAZ) regions. In addition, they stated a formation of partially heat-affected zone (PHAZ) between the transition zones and the base material. Furthermore, they found that the heterogeneous thermoplastic flow changed depending on the material properties. On the other hand, Yilbaş [8] emphasized the importance of rotational speed in order to create sufficient deformation at the interface in the FW method. Mercan et al. [9] used the FW method to join steel materials and emphasized that the increase in rotational speed would increase the heat input and the importance of heat input for plastic deformation at the interface. Mohammed et al. [10] determined that the strength and hardness of the samples joint using the FW method increased depending on the increase in heat input. Joining different material pairs using MLM is a method performed in solid phase as in FW and FSW joining methods. Yani et al. [11] reported that the joint type and quality in solid phase processes were directly related to the heat production produced by the plastic flow in their study which they conducted using the FSW method. Therefore, they applied a model for plastic flow by applying the principle of fluid dynamics along with the relationship between viscous moment and viscosity in the metastable state welding stage. They proposed a new calculation method for viscoplastic heat generation in the FSW process. Huang et al. [12], used FSW as the method and emphasized the importance of the number of revolutions examined in joining different metal pairs, which is the subject of the current study. Moghaddam et al. [13], reported that as a result of the increase in the weld temperature of brass plates joined using FSW, the density of mixing bands consisting of ultra-fine grains increased, which in turn increased tensile and yielding strengths. Barlas [14], who joined friction stir spot welding with CuZn30 brass and DP600 steel pair, determined recrystallization and a softening in the brass material and an increase in the hardness of the weld metal. In another study using FSW, Barlas [15], stated that attention should be paid to hardness and deformation when fixing materials. Xiao et al. [16], investigated the deformation characteristics of H62 brass. Their results indicated that while the flow stress of H62 brass and the strain rate increased, the deformation temperature decreased. Başdemir et al. [17], reported that the stress concentration and hardness values increased due to deformation in regions with high cross-sectional changes in cold forging plastic forming processes. Liu et al. [1], stated that parallel twins occurred as a result of plastic deformation in brass materials and hardness values increased due to grain refinement.

Altınbalık et al. [18], stated that in extrusion type forging processes, different geometries with the same cross-sectional area made differences in flow difference and flange dimensions. Jose et al. [19], reported that metals could be modeled with plastic strain flow formulation. Luo et al. [20], joined H90 brass and D60 steel using radial friction method. They found that Fe and Cu elements diffusion appeared at the welding interface.

This study used MLM, a joining method, which has not been used in today's manufacturing methods until now. This method allowed joining AISI 1040 and CuZn30 material pairs using different parameters. The study examined microstructural change and mechanical properties of the joined samples. The results indicated that MLM could be used in joining material pairs that cannot be joined using other joining methods. The researcher believes that MLM, as a newly developed method, is an environmentally friendly method that can be widely used in joining technology in the near future. With this in mind, the current study will make important contributions to the literature because, for automobile components that require an interlayer in the joining process, such as ball joints, turbocharger shafts, clutch hub and axle housing, where the FW method is popularly used [21], joining processes can be done without using an interlayer. Furthermore, MLM can be used in the production of parts such as tie rod ends, which are joint using the spinning method, which is a difficult and expensive method to manufacture for the automotive industry.

2 Experimental Procedures

2.1 Sample Preparation

The schematic view of the joined samples using MLM is given in Fig. 1. The part to be reshaped was manufactured in dimensions that would ensure the friction movement in the mold and fill the channel as a result of plastic deformation.

This part was produced cylindrically via lathe. The volume of the duct was calculated by the formula (1) and the part size (H) to be reshaped in accordance with the determination of the obtained value. To examine the applicability of the mechanical locking process, errors and dimensional deviations that might had occurred due to thermal expansion and pressure were ignored within the scope of this study.

Equation 1 is used to match the volume of the two parts to be joined. While “h” shows the depth of the mold cavity, “a” shows the mouth width of mold, “b” shows the base width of mold, and “H” shows the length of the piece to be reshaped. “R” is the initial diameter of the reshaped part and is regarded to be equal to the value of “a”, which refers to the mold mouth width.

$$h \left(\frac{a^2 + ab + b^2}{2} \right) = \pi H \left(\frac{r^2}{2} \right) \quad (1)$$

There are a number of parameters that affect the joining properties, especially when joining different metal types using different methods. The amount of heat generated in the selection of parameters has an impact on a wide range, such as microstructures in the welding area, the geometries of the microstructure forming the connection metal region, the types and sizes of possible defects, the amount and shape of various intermetallic compounds [22]. MLM has the similar parameters. Depending on the number of revolutions, the heat generated during friction directly affects the amount of material that will undergo plastic deformation, the microstructure and the material flow. Therefore, this study has determined the number of revolutions, which has an important effect on the amount of heat, as a variable parameter. Table 1 shows the selected parameters. Parameters and sample sizes were determined through preliminary experiments after a careful review of the related literature. The related literature states that hot pressing interferes with oxide film formation and diffusion mechanisms by increasing forward axial pressure

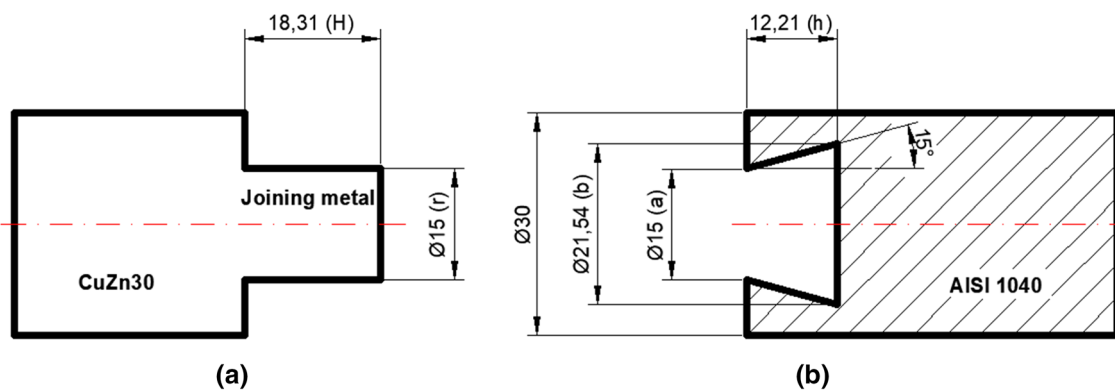


Fig. 1 Sample sizes used in mechanical locking method (mm). (a) Reshaped metal (b) Mold metal

Table 1 The process parameters for MLM

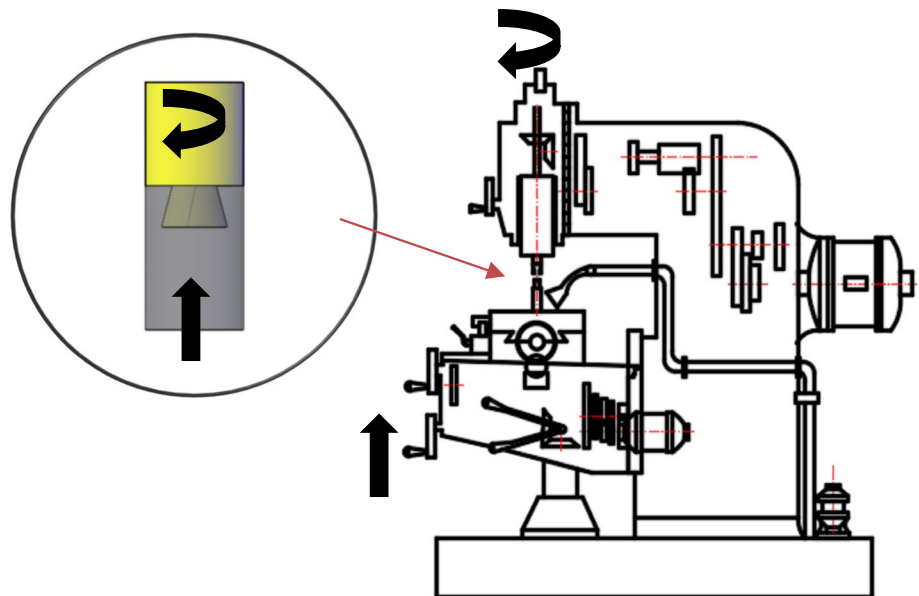
	S1	S2	S3
Rotation speed (rpm)	900	1120	1400
Feed rate (mm/min)	16		
Joining angle	15		

[23]. The feed rate should be selected at a sufficient size to ensure a regular material flow and not to cause buckling. In addition to these results that will occur due to progress, the process should be completed quickly considering the heat losses, and the brass material should be filled into the mold with the aid of sufficient pressure. Another parameter should also be considered to allow the material flow into

the cavity. This parameter is the joint angle, which should be large enough to provide appropriate movement to form the flange. Considering the machine limits, the parameters are selected as follows.

The joining processes were completed at the Taksan FU315 × 1250 brand/model milling machine. Figure 2 shows the joining method and the schematic picture of the machine.

Tables 2 and 3 show the chemical compositions of the metal alloys based on spectrometric analysis results. Table 4 also represents the physical properties of the samples.

Fig. 2 The schematic picture of mechanical locking method and machine**Table 2** Chemical composition of AISI 1040 (wt.%)

	C	Mn	Si	Mg	Cu	S	Al	Fe
AISI 1040	0.42	0.55	0.30	–	–	0.035	–	Bal

Table 3 Chemical composition of CuZn30 (wt.%)

	Cu	Zn	Pb	Sb	Bi	P	Fe
CuZn30	71.8	28.2	≤% 0.03	≤% 0.05	≤% 1.002	≤% 0.01	≤% 0.10

Table 4 Properties of the AISI 1040 steel and CuZn30 brass

	Tensile Strength (MPa)	Density (g/cm ³)	Thermal expansion Coefficient (μ K ⁻¹)	Thermal conductivity [W/(mK)]	Melting point (°C)	Percentage of linear shrinkage (%)
AISI1040	520–620	7.82	11.5	52	1470	12
CuZn30	206–290	8.85	18.1	115	1056	–

2.2 Microstructure Characterization

The samples were mechanically polished with abrasive paper, and then electrolytically polished at room temperature. The surface analysis of all samples were examined by scanning electron microscope equipped with secondary electron and backscattered electron detectors (SEM SE-BSE, Tescan® Mira3 XMU, Brno, Czechia).

Hardness measurements were made in three different directions shown as a, b and c in Fig. 8 along the contact line at the interfaces of the joined samples. Hardness measurements continued until they reached the matrix materials. The measurements were completed under a load of 100 g with a holding time of 13 s using the Qness Q10 hardness tester.

2.3 Mechanical Properties

Tensile test samples were prepared according to TS EN ISO 6892–1/March 2011 standards. The schematic picture of the tensile test sample is shown in Fig. 3. The tensile tests were conducted by a Shimadzu testing machine at a strain rate of $1 \times 10^{-3} \text{ s}^{-1}$, and a contacting Instron extensometer was used

to measure strain when the sample was loaded. The smallest diameter value (15 mm) forming the joint was used in calculating the stress values.

3 Experimental Results

3.1 Macro Structure

Macro and interface photos of samples joined using MLM are given in Fig. 4. The joining process was carried out until the volumetric fit was filled the cavity up successfully. Depending on the joint design, the friction surface remains inside the AISI 1040 material and the heat-affected zone (HAZ) is only seen on the AISI 1040 steel material side due to the difference between the heat conduction coefficients of the materials (Table 3 and Fig. 3). HAZ increased as the number of revolutions increased and reached the highest value in sample no S3.

Although Ma et al. [24], have investigated different microstructures affecting the mechanical properties of the parts joined using the FW method and reported to exist at

Fig. 3 The schematic illustration of tension test samples

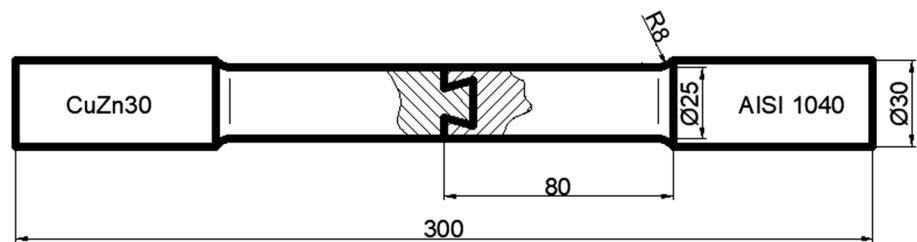
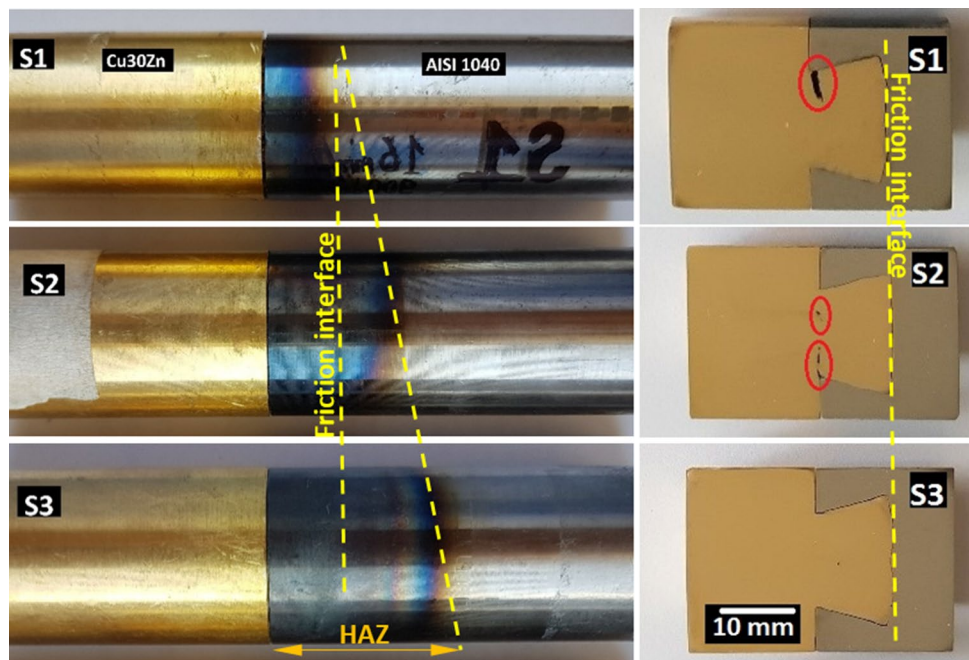


Fig. 4 The macro photos of the samples after joining (HAZ) and intersection of joints



the interface, they have reported that the heat effect caused by the friction in the formation of microstructures varies depending on the number of revolutions. They have also stated that plastic deformation occurs faster and easier depending on the increasing amount of heat. Brass material plastic deformation became easier with the increasing temperature in sample S3. As a result, the brass material filled the mold cavity more quickly [16].

The pressures occurring on both sides of the friction interfaces were almost the same, but the thermal conductivities, melting point yield strengths and other mechanical properties of AISI1040 and CuZn30 materials were different as shown in Table 3. For this reason, the total physical properties of the materials, melting point incompatibility and especially the connection design were responsible for the increase in the HAZ region on the steel side. In addition, the plastic deformation capability of brass is better than steel, and steel has higher yield strength than brass. Because of these differences, plastic deformation almost completely occurred on the CuZn30 side (Fig. 4). The excessive plastic deformation on the CuZn30 side was a result of the high heat generated by friction. The resulting amount of heat provided enough thermoplastic state brass to form the joint metal [20].

Figure 4, which describes the sample interface macro images, shows that porosity occurs in samples S1 and S2 in the parts shown in the circular area on the joint metal. The lack of sufficient heat and pressure caused porosity in samples S1 and S2 due to insufficient material flow [2, 25] because the dynamic brass flange with the thermoplastic flow (in the free and viscoplastic state) formed by the effect of axial pressure force flows from the friction interface towards the cavities in the mold and separates from the friction interface. The thermal conductivity and mechanical properties of both materials are determinant in the flow of materials [15]. The brass, which was directed from the friction interface, was forged by other flowing material (the brass that filled the cavity and separated from the steel interface was subjected to forging-like process). However, thermoplastic brass with a dynamic flow state cannot be produced sufficiently from the joint interface [20]. Therefore, the deformation ability of the joint metal, which consists of brass flanges with low temperature due to heat loss, decreases over time [22]. As a result, some groove-shaped gaps occur due to plastic deformation at the interface due to insufficient heat and insufficient material flow [2].

The cavities formed in the parts subject to plastic deformation and in the region where the conic section narrowed did not occur in the S3 sample. On the other hand, the increasing amount of heat in the sample S3 due to the increase in the number of revolutions prevented the formation of porosity. This situation occurred as a result of the metal flow that occurred in the form of flange formation at a higher temperature than other samples. This may be

attributed to the decreased yield strength for easier plastic deformation. The flow of the brass alloy (S3) reduced the dislocation density, and recrystallization of the alloy was achieved with the recovered grains. Avadhanam et al. [7], have stated that the recovered grains are obtained with the effect of pressure and material flow formed radially and axially, and this is the reason for the differences in microstructure. The small difference between the grain sizes in sample S3 in the microstructure examinations confirmed this situation (Fig. 6). As a result of the increase in the number of revolutions, the resulting porosity decreased with the steady flow occurring in the rising temperature value and completely disappeared in sample S3.

3.2 Microstructural Characterization

The original microstructures of CuZn30 brass and AISI 1040 steel are shown in Fig. 5a, b, and both are homogeneous microstructures. The average grain sizes measured by the line intercept technique were about 16 μm for steel and 20 μm for CuZn30 brass. Both AISI 1040 steel and CuZn30 brass equiaxed coarse grains with similar grain sizes.

The microstructures in the joint metal characterized by SEM are shown in Fig. 5 to reveal the deformation behaviors of grains. Thermoplastic brass becomes droved and flowed from the joint interface with the effect of axial pressure. This situation provides the flange formation just like friction welding and is completed by the flange taking its form in the mold.

Heavy deformation of brass and high temperature ($> 700\text{C}$) induce $\beta \rightarrow \alpha$ phase transformation. The transformed α phase diffuses into a fine needle, and the volume ratio increases with increasing deformation temperature, which helps to improve the plasticity of the brass [16]. However, the temperature of the steel/brass mechanical locking joint drops rapidly while the process continues, thus making recrystallization difficult for thermoplastic brass [20]. As a result, refined grains are formed in different sizes along with the joint metal. During the process, the grains with different thermal properties and heterogeneities occur [7], and the researcher believes that in MLM process, these grains are exposed to different pressure values depending on the space in the channel. This situation causes different grain sizes. On the other hand, the unequal thermal distribution caused by friction causes some grains to grow abnormally, and it eventually causes the microstructure to deteriorate the homogeneity (Fig. 5) [16].

As can be seen from the SEM photographs, the middle part of joint metal consisted of coarser brasses as in the main material (Fig. 5c, d and e), while the parts close to the surface of the joint metal consisted of finer brasses (Fig. 5f, g and h). This was a result of the rapid removal of heat in the parts close to the joint interfaces and the increased pressure

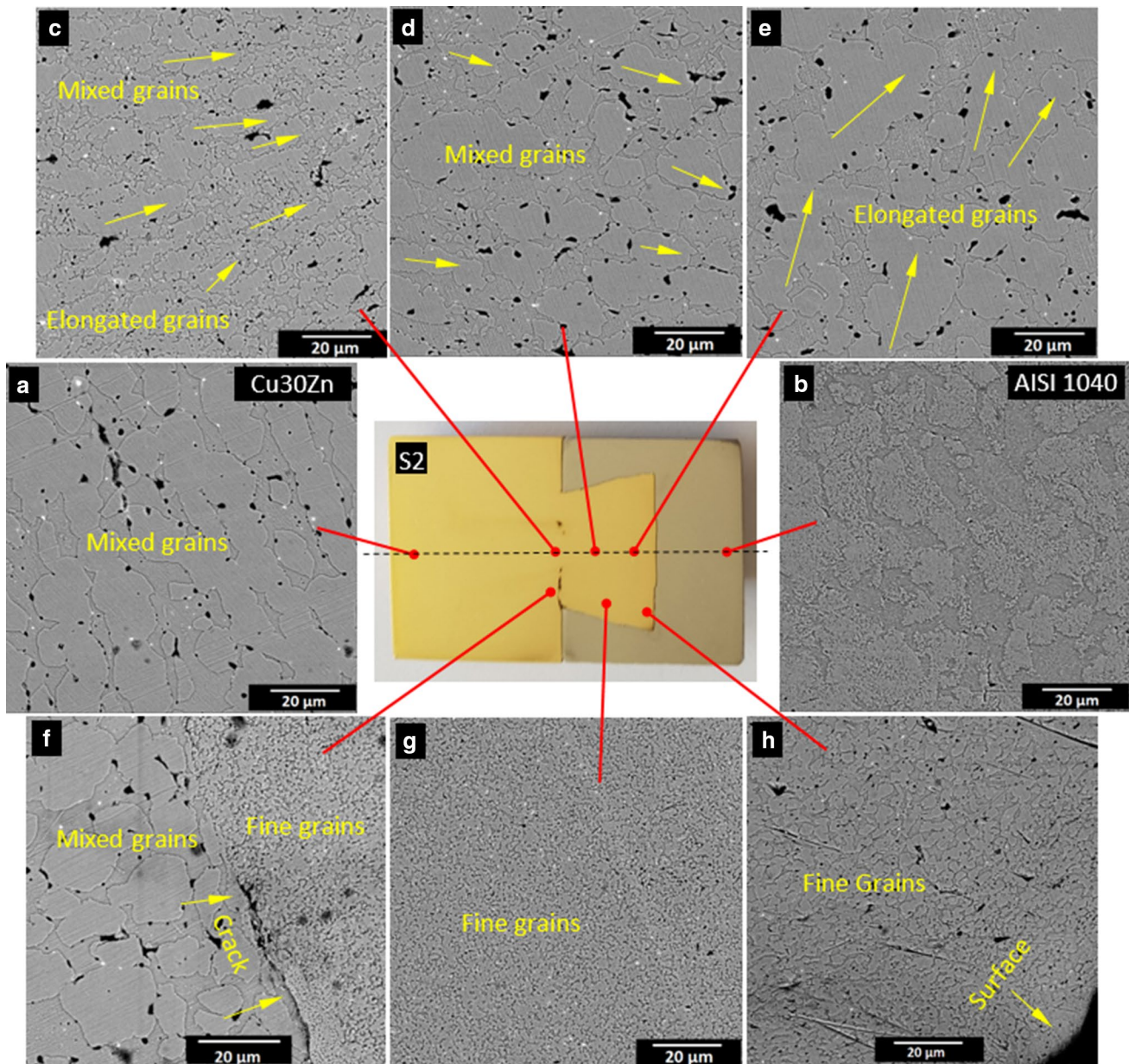


Fig. 5 SEM images of the sample microstructure no S2 (a) CuZn30 brass originally microstructures, (b) AISI 1040 steel originally microstructures (c, d and e) Mixing regions of the joint metal, f, g and h) Flow regions of the joint metal

effect due to the material flow created as a result of friction and axial pressure in the same parts. The literature illustrates that the microstructure differences occur due to the flow differences in materials undergoing plastic deformation due to various reasons [18]. On the other hand, there is a difference in microstructure between Fig. 5g and h. The researcher believes that this situation occurs due to the difference between the contact areas at the interface and the pressure differences due to the material flow, and the pressure is a more effective mechanism because the microstructure formed in Fig. 5g is similar until the crack shown in Fig. 5f.

In the region shown in Fig. 5h, the interface is wider, and the researcher expects a finer grain structure in this region due to the higher cooling rate. However, a finer grain structure occurred in the region shown in Fig. 5g. This shows that the pressure effect is greater in this region and the material flow occurs from Fig. 5h–f and the pressure rises in these regions, resulting in a finer grain structure.

Figure 5c shows the deformation of the rice grains due to axial pressure. The equiaxed grains (Fig. 5d) were formed in the advancing direction at the interface due to hot deformation. The subsequent deformation forced the material to

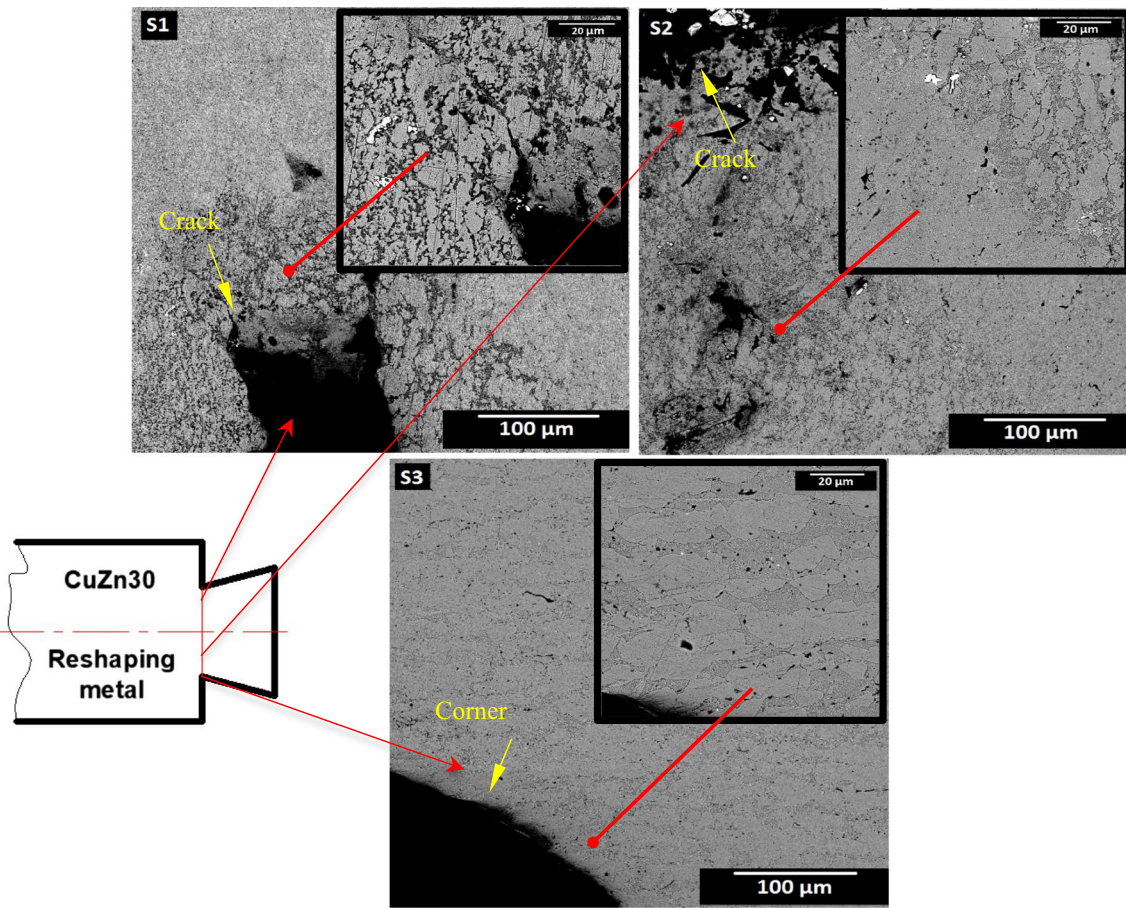


Fig. 6 Parts where the joint metal sections are the narrowest in samples S1, S2 and S3

change the flow direction at the interface due to the friction between the mold and the brass alloy (Fig. 5e).

Figure 5f shows that the grains got smaller as they got closer to the joint interface, but coaxial medium-sized grains were seen in the part below the joint interface. Figure 5f shows the equiaxed and mixed size grains at the link metal interface. In this region, fine grains and coarse grains are separated from each other by a hot cracking line. The main metal side still had coarse grain structure, which may mean that no temperature related to re-formation occurred on out-cavity grains. Avadhanam et al. [7], have clearly reported that there is near-complete dynamic recrystallization (DRX) in the thermoplastically deformed region in FW, which causes grain refinement. The fine grain structure shows the recrystallized grains with high dislocation density by cold deformation at the interface. Figure 5g shows the region with fast cooling rate and cold deformation that caused the finest grain structure, while heat dissipation in the middle of the cavity led to coarse grains as in Fig. 5d and 4e. As it can be clearly seen from the deformation directions of the grains in this area, fine grains do not change their direction and these

grains form the grains as seen in Fig. 5g by flow of material within cold deformation.

In Fig. 5f, the recrystallized fine grains in the upper part and the medium-sized grains, which shrink with the deformation effect and are distributed almost equiaxially, are seen together. The grain size incompatibilities have led to the crack formation. The researcher observed that the crack formation did not occur along the whole of the grain size incompatibilities, and the cracks started from the corner points and ended by progressing a little along a straight line. Cracks were formed in almost the same regions in samples S1 and S2. However, the researcher observed that there was no crack in the sample no. S3 and the grain size incompatibilities decreased due to the increasing amount of heat (Fig. 6). The material flows occurred similarly in all three samples, regardless of their rotational speeds.

SEM pictures of the part where the cross-section was the narrowest (where cracks were formed) in the joint metals of the samples were numbered S1, S2 and S3 are given in Fig. 6. Cracked parts and deformed grain directions are clearly seen in SEM images. The parts from which SEM

images were taken in all three samples are shown on the schematic picture given in Fig. 6.

As it can be clearly seen, S1 and S2 had granular incompatibilities in both their directions and their grain sizes. This led to the formation of cracks with the conversion of hot deformation to cold deformation along the steel interface. These incompatibilities did not occur for sample S3, therefore, there were no cracks in similar regions of S3. A smooth grain transformation increases the compatibility of grains, and mixed grain size region also supports the heat exchange capacity by relieving the thermal stress on grains. Moreover, by increasing rotation speed, more frictional heat was generated, and the joint interface temperature increased accordingly. This resulted in intensive mixing of the joint metal and reduced the effects of crack formation by reducing the incompatibility between the grains [22]. Increased heat for S3 increased grain size even at the near-steel mold cavity interface and reduced granular mismatch, resulting in lower crack initiation sensitivity that prevented crack propagation.

The literature reported that furrow-shaped holes were formed at the joint boundary line in copper steel pairs joined using friction welding method [20]. Similarly, the current study determined that similar gaps occurred and there was no diffusion between steel and brass when joining AISI 1040 steel and CuZn30 brass material pairs using MLM (Fig. 7).

As a result of the lack of diffusion, the joint material pair was movable in a direction perpendicular to the axis of symmetry with the decrease of heat on them after joining. The amount of diffusion depends on the operating parameters and it varies according to the temperature and joining type [26, 27].

3.3 Microhardness Distributions

Average hardness values for AISI 1040 and CuZn30 are 220 HV, 134 HV, respectively. Since similar hardness

distribution changes were observed among the joint samples, the values of the sample S3 with the highest hardness distribution change were used. Hardness measurements were completed on both sides from the joint interface, in three different directions parallel to the symmetry axes and to each other (Fig. 8). Thus, the study determined microhardness changes on the friction surface and side surfaces.

When the microhardness profiles obtained from three directions were compared with each other, it was observed that the line close to edge, which is illustrated as (a), had the highest hardness value, and the lines close to symmetry axis (b) and (c) had lower hardness values. This situation may be attributed to the cooling rate and deformation. An evaluation made in the direction of Fig. 8c (along the axis of symmetry) revealed that the microhardness values decreased in the regions close to the friction interface (Fig. 5e) with the effect of friction heat. This evaluation also indicated that the microhardness increased due to the increasing cooling rate (Fig. 5d and c) towards the base metal on the same axis.

The literature confirms that grain refinement increases hardness [1, 28]. The hardness of the joint metal increases due to the thinning of the grains under relatively lower heat input conditions [29]. Hardness in the joint metal was measured at a maximum of 138 HV and a minimum of 120 HV. This change may be associated with grain thinning and increased dislocation due to the excessive deformation they were subjected to when the samples were joined. The finer particles close to the interface in SEM-BSE images confirm this situation (Fig. 5f, g and h). Microhardness measurements support these differences in distinguishing the different parts seen in joint metal microstructure SEM investigations and shown in Fig. 5.

Transformation of grains or microstructure, which was seen at or around interface, did not cause any significant change in microhardness value of AISI 1040. Increasing

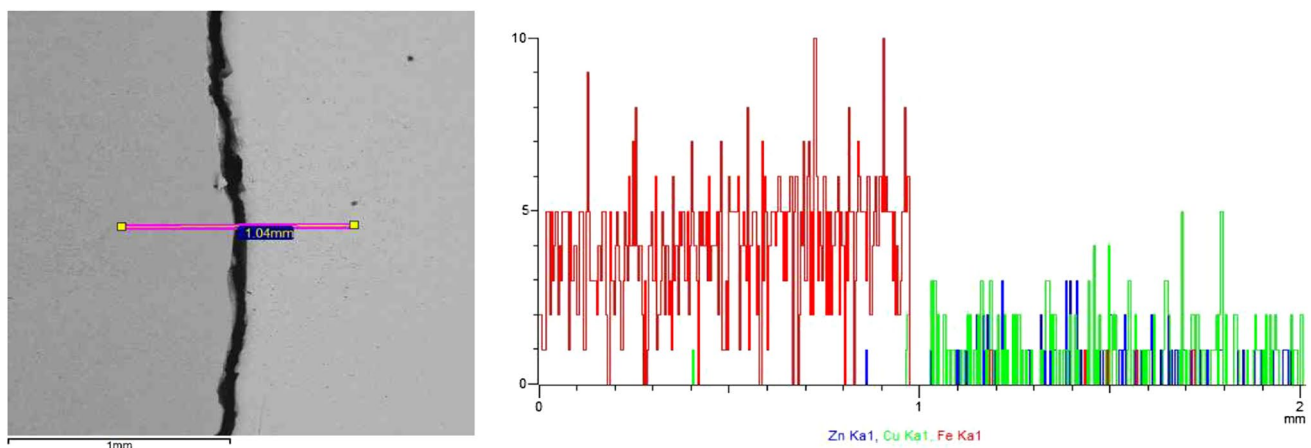
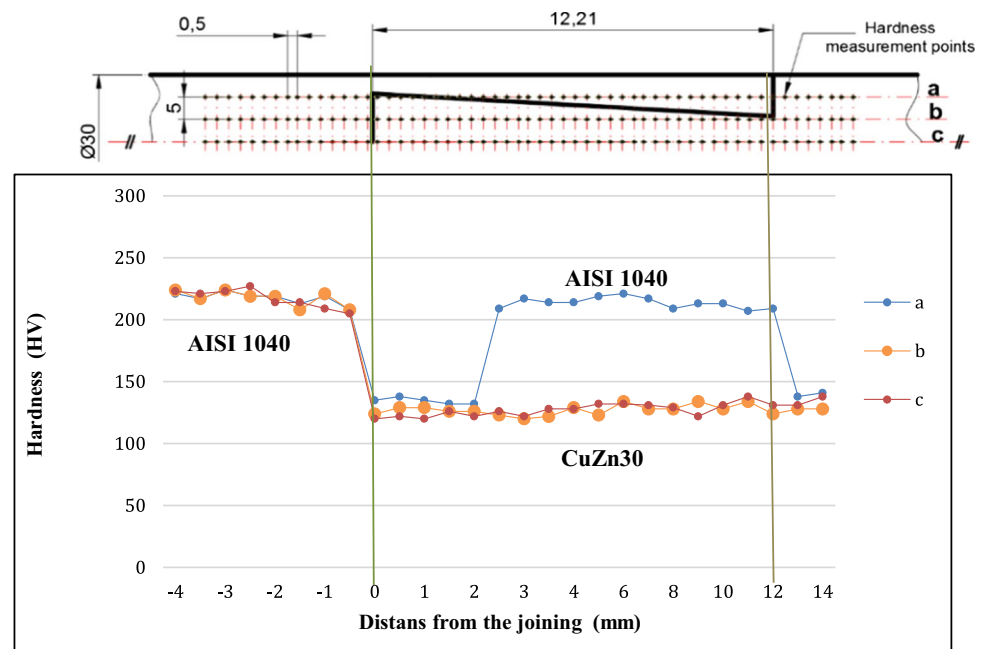


Fig. 7 The SEM–EDX elemental line analysis of the joint interface

Fig. 8 Microhardness distributions of joint interface (mm)



temperature increased the HAZ zone and reduced the hardness close to the steel interface to 205 HV.

3.4 Tensile Properties

Macro photographs of the samples broken as a result of the tensile testing are shown in Fig. 9. Sample S1 was broken approximately 1 mm above the narrowest part of the joint metal in the direction of crack propagation shown in Fig. 4. Sample S2 was damaged in the form of a straight line along the crack shown in Fig. 4 and at the narrowest part of the joint metal. Cracks formed during the joining process were the main cause of damage in both samples. In the sample no.

S3, the damage occurred in a straight line from the end point of the plastic deforming part. The damage in the sample no. S3 was in the region where the cross-section narrowed. This was an expected result in terms of joint quality. The results of the tensile tests indicated that all three samples were suddenly broken without necking.

Figure 10 shows the tensile test results of the main materials and the joint samples with their standard deviation values. Tensile values for AISI 1040 and CuZn30 were measured as 522 MPa and 280 MPa, respectively. Tensile values were measured as 19.9 MPa for the joint sample S1, 181.99 MPa for the joint sample S2 and 265.88 MPa for the joint sample S3.

Fig. 9 Samples broken as a result of the tensile test



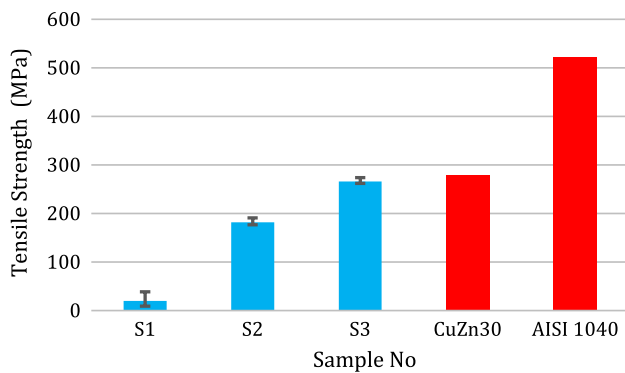


Fig. 10 The result of the tensile test

When their numbers of revolutions were compared, the heat values arising on the samples no. S1 and S2 were lower than the sample no. S3. Comparison in terms of their numbers of revolutions indicated that the heat values arising on samples S1 and S2 were lower than the value of sample S3. This caused CuZn30, which was forced to plastic deformation and directly affected the mechanical test values, to be forced into an inhomogeneous plastic flow and pore formation on both samples as stated in the literature. As a result of the low thermal value on the samples, the residual stresses occurring as a result of the rapid cooling rate and a large temperature gradient affect the mechanical values negatively [30]. On the other hand, as a result of combination of anisotropic behavior caused by solidification of microstructure in the direction seen in Figs. 5, 6 and other specified effects in samples S1 and S2, their mechanical properties were significantly lower. Along with these, the decrease in mechanical properties was an expected result since stress concentrations were formed in parts with sudden cross-section changes depending on the part geometry.

This study measured the tensile strength of the samples and found a small decrease of 4% between the base material and the strength of sample S3. However, this was not achieved by diffusion, but only as a result of mechanical bonding. The current study determined that as a result of the changes made in the parameters, the strength increased significantly in the samples S2 and S3 compared to the sample S1. Therefore, using parameters that are compatible with each other can further increase the strength of the joining.

The changes made in the parameters increased the strength of sample S3 significantly compared to the other samples. Although 4% less mechanical test results were obtained in sample S3 (265.886 MPa) compared to the base material strength values (280 MPa), it is clearly seen that the mechanical properties can be increased using MLM method with the help of the changes in the joint geometry.

Due to the increase in rotation speed, high deformation temperature improves ductility by decreasing the yield strength

and increases grain coordination and plasticity [16]. Samples coded as S1 and S2 did not have too much heat input, however, lower rotation speed caused the crack formation, which is the most important reason of deterioration in mechanical properties. By increasing rotation speed for S3 sample, the sufficient heat input can be the optimum parameter for appropriate mechanical properties close to main material's tensile strength.

4 Conclusion

MLM is a new joining method. It can be used successfully especially in the joining of different metal pairs. The results of the examinations made on the method led the researcher to believe that it can be used in industrial applications. Investigations are ongoing for joining Steel/Copper metal pairs using MLM and joining automobile axle shaft flange connections. In this study, the researcher joined AISI 1040 steel and CuZn30 brass using a novel patented method named mechanical locking method for the first time. Following conclusion can be derived from this study:

- Materials that have different chemical and physical properties and cannot be joined using other methods such as casting and welding can be joined using the mechanical locking method.
- In samples no S1 and S2, which were joined at 900 and 1120 rpms, respectively, cracks were formed in the parts where the cross-section was narrow. Cracks were formed due to incompatibility between grains caused by low temperature low speed.
- Hardness in the joint metal was measured at a maximum of 138 HV and a minimum of 120 HV. This change was associated with grain thinning and increased dislocation due to the excessive deformation they were subjected to when the samples were joined.
- The amount of heat obtained with increasing number of revolutions (1400 rpm), as in sample S3, prevented crack formation by providing a soft grain transformation.
- The increase in the number of revolutions made the material flow and microstructure more regular in sample S3. This also provided the highest tensile test results as 265.88 MPa in the sample S3. This value is 4% lower than the main material.
- The optimization of locking parameters for improving the mechanical properties should be studied in the near future both experimentally and computationally.

References

1. Liu, L., Wang, J., & Zhou, J. (2019). Characterization and analysis on micro-hardness and microstructure evolution of brass

- subjected to laser shock peening. *Optics & Laser Technology*, 115, 325–330. <https://doi.org/10.1016/j.optlastec.2019.02.043>
2. Sun, Y. F., Xu, N., & Fujii, H. (2014). The microstructure and mechanical properties of friction stir welded Cu–30Zn brass alloys. *Material Science and Engineering: A*, 589, 228–234. <https://doi.org/10.1016/j.msea.2013.09.094>
 3. Mohorana, B. R., Sahu, K. S., Sahoo, K. S., & Bathe, R. (2016). Experimental investigation on mechanical and microstructural properties of AISI 304 to Cu joints by CO₂ laser. *Engineering Science and Technology, an International Journal*, 29(19), 2684–2690. <https://doi.org/10.1016/j.jestch.2015.10.004>
 4. Magnabosco, I., Ferro, P., Bonollo, F., & Arnberg, L. (2006). An investigation of fusion zone microstructures in electron beam welding of copper–stainless steel. *Material Science and Engineering: A*, 424(1–2), 163–173.
 5. Mercan S. (2017). Mechanical locking method, Turkish Patent and Trademark Office. No: TR 2015 03256 B 2017/05/22.
 6. Mercan, S. (2019). Joining of dissimilar metal pairs by mechanical locking method. *Gazi University Journal of Science Part C*, 7(1), 25–36. <https://doi.org/10.29109/gujsc.437488>
 7. Avadhanam, S. K., Khadeer, S. A., Rajinikanth, V., Pahari, S., & Kumar, B. R. (2021). Evaluation of bond interface characteristics of rotary friction welded carbon steel to low alloy steel pipe joints. *Materials Science and Engineering: A*, 824, 141844. <https://doi.org/10.1016/j.msea.2021.141844>
 8. Yilbaş, B. S., Şahin, A. Z., Kahraman, N., & Al-Garni, A. Z. (1995). Friction Welding of St-Al and Al-Cu Materials. *Journal of Materials Processing Techn.*, 49(3–4), 431–443. [https://doi.org/10.1016/0924-0136\(94\)01349-6](https://doi.org/10.1016/0924-0136(94)01349-6)
 9. Mercan, S., Aydin, S., & Özdemir, N. (2015). Effect of welding parameters on the fatigue properties of dissimilar AISI 2205–AISI 1020 joined by friction welding. *International Journal of Fatigue*, 81, 78–90. <https://doi.org/10.1016/j.ijfatigue.2015.07.023>
 10. Mohammed, A., & M., Kulkarni, A., S., Sathiya P., Sunkulp, G. (2015). The impact of heat input on the strength, toughness, microhardness, microstructure and corrosion aspects of friction welded duplexstainless steel joints. *Journal of Manufacturing Processes*, 18, 92–106. <https://doi.org/10.1016/j.jmapro.2015.01.004>
 11. Yan, F., Zhang, Y., Shen, J., Fu, X., & Mi, S. (2021). A new calculation method of viscoplastic heat production generated by plastic flow of friction stir welding process. *Materials Chemistry and Physics*, 270, 124795. <https://doi.org/10.1016/j.matchemphys.2021.124795>
 12. Huang, G., Feng, X., Shen, Y., Zheng, Q., & Zhao, P. (2016). Friction stir brazing of 6061 aluminum alloy and H62 brass: Evaluation of microstructure, mechanical and fracture behavior. *Material & Design*, 99, 403–411. <https://doi.org/10.1016/j.matdes.2016.03.094>
 13. Moghaddam, M. S., Parvizi, R., Haddad-Sabzevar, M., & Davoodi, A. (2011). Microstructural and mechanical properties of friction stir welded Cu–30Zn brass alloy at various feed speeds: Influence of stir bands. *Material & Design*, 32(5), 2749–2755. <https://doi.org/10.1016/j.matdes.2011.01.015>
 14. Barlas, Z. (2017). Weldability of CuZn30 Brass/DP600 steel couple by friction stir spot welding. *Acta Physica Polonica A*, 132(3–11), 991–993. <https://doi.org/10.12693/APhysPolA.132.991>
 15. Barlas, Z. (2015). Effect of friction stir spot weld parameters on Cu/CuZn30 bimetal joints. *The International Journal of Advanced Manufacturing Technology*, 80(1), 161–170.
 16. Xiao, Y., Guo, C., & Guo, X. (2011). Constitutive modeling of hot deformation behavior of H62 brass. *Material Science and Engineering: A*, 528(21), 6510–6518.
 17. Başdemir, V., Baygut, A., & Çulha, O. (2018). Plastic forming technologies used in fastener manufacturing with cold forming technique. *Journal of Advanced Technology Science*, 7(3), 18–28.
 18. Altunbalık, T., & Çan, Y. (2009). Influence of the die geometry on load and metal flow in extrusion-forging processes. *Trakya University Journal of Natural Sciences*, 10(1), 1–8.
 19. Bressan, J. D., Martins, M. M., & Button, S. T. (2017). Analysis of metal extrusion by the finite volume method. *Procedia Engineering*, 207, 425–430. <https://doi.org/10.1016/j.proeng.2017.10.799>
 20. Luo, J., Xiang, J., Liu, D., Li, F., & Xue, K. (2012). Radial friction welding interface between brass and high carbon steel. *Journal of Materials Processing Technology*, 212(2), 385–392. <https://doi.org/10.1016/j.jmatprotec.2011.10.001>
 21. Balasubramaniana, M., Murali, S., Hemadri, C., & Kumar, R. (2021). A new method of dissimilar friction welding of titanium to stainless steel. *Materialstoday Proceedings*, 46(9), 3644–3647. <https://doi.org/10.1016/j.matpr.2021.01.675>
 22. Khodaverdizadeh, H., Mahmoudi, A., Heidarzadeh, A., & Nazari, E. (2012). Effect of friction stir welding (FSW) parameters on strain hardening behavior of pure copper joints. *Material & Design*, 35, 330–334. <https://doi.org/10.1016/j.matdes.2011.09.058>
 23. Arık, H., Semerci, P., & Kırmızı, G. (2017). Investigation of wear behavior of aluminum matrix composite reinforced by Al₂O₃ and produced by hot pressing process. *Gazi University Journal of Science Part C*, 5(4), 87–97.
 24. Ma, H., Qin, G., Dang, Z., & Geng, P. (2021). Interfacial microstructure and property of 6061 aluminium alloy/stainless steel hybrid inertia friction welded joint with different steel surface roughness. *Materials Characterization*, 179, 111347. <https://doi.org/10.1016/j.matchar.2021.111347>
 25. Erdem, M. (2015). Investigation of structure and mechanical properties of copper-brass plates joined by friction stir welding. *The International Journal of Advanced Manufacturing Technology*, 76(9–12), 1583–1592. <https://doi.org/10.1007/s00170-014-6387-1>
 26. Atasoy, E., & Kahraman, N. (2008). Diffusion bonding of commercially pure titanium to low carbon steel using a silver interlayer. *Material Characterization*, 59(10), 1481–1490. <https://doi.org/10.1016/j.matchar.2008.01.015>
 27. Cheng, X., Bai, B., Gao, Y., Fu, H., & Xing, J. (2010). Microstructural characterization and properties of Al/Cu/steel diffusion bonded joints. *Metals and Material International*, 16(4), 649–655. <https://doi.org/10.1007/s12540-010-0820-2>
 28. Ren, C. X., Wang, Q., Zhang, Z. J., Yang, H. J., & Zhang, Z. F. (2019). Enhanced tensile and bending yield strengths of 304 stainless steel and H62 brass by surface spinning strengthening. *Material Science and Engineering: A*, 754, 593–601.
 29. Shen, J. J., Liu, H. J., & Cui, F. (2010). Effect of welding speed on microstructure and mechanical properties of friction stir welded copper. *Material & Design*, 31(8), 3937–3942. <https://doi.org/10.1016/j.matdes.2010.03.027>
 30. Robinson, J. S., & Redington, W. (2015). The influence of alloy composition on residual stresses in heat treated aluminium alloys. *Material Characterization*, 105, 47–55. <https://doi.org/10.1016/j.matchar.2015.04.017>

Publisher's Note Springer Nature remains neutral with regard to jurisdictional claims in published maps and institutional affiliations.



Serdar Mercan was born in Sivas/Turkey in 1975. He completed his undergraduate education at Gazi University, Faculty of Technical Education, Department of Mechanical Education (1994-1998). He completed his graduate studies at Cumhuriyet University, Institute of Science and Technology, Department of Mechanical Engineering (1999-2002). He completed his doctoral studies in the Department of Metallurgy Education (2009-2013) at the Firat University, Institute of Science and Technol-

ogy. He continues his studies as a faculty member at Sivas Cumhuriyet University, Faculty of Technology, Mechatronics Engineering,

Mechanical Systems. He was appointed as the general manager of Sivas Technology Development Zone Founder and Operator A.Ş. in 2016 and continues to work. He has 3 Technical Books, 10 international articles and 9 papers published. It was deemed worthy of 5 TÜBİTAK awards, 1 institution acknowledgment certificate, 1 Ministry of Industry and Technology award. He is a class A occupational safety specialist and works with CAD, CAM and CAE package programs as well as academic and scientific studies. He does beekeeping as a hobby. He is married and has two children.